JOURNAL OF NANO- AND ELECTRONIC PHYSICS
Vol. 8 No 2, 02026(5pp) (2016)
ЖУРНАЛ НАНО- ТА ЕЛЕКТРОННОЇ ФІЗИКИ
Том 8 № 2, 02026(5cc) (2016)

Spray Deposited Nanocrystalline ZnO Transparent Electrodes: Role of Precursor Solvent

C.M. Mahajan[1,2,*], M. Pendharkar[1], Y.A. Chaudhari[3], S.S. Sawant[1], B. Ankamwar[4], M.G. Takwale[2]

[1] *Department of Engineering Sciences and Humanities, Vishwakarma Institute of Technology, Pune – 411 037, India*
[2] *School of Energy Studies, Savitribai Phule Pune University – 411 007, India*
[3] *Department of Physics, Shri Pancham Khemaraj Mahavidyalaya, Sawantwadi – 416 510, India*
[4] *Department of Chemistry, Savitribai Phule Pune University, Ganeshkind, Pune – 411007, Maharashtra, India*

(Received 21 March 2016; revised manuscript received 10 June 2016; published online 21 June 2016)

Nanocrystalline ZnO thin films were deposited by intermittent spray pyrolysis using different alcoholic and aqua-alcoholic precursor solvents. The XRD analysis reveals the polycrystallinity of hexagonal wurtzite type ZnO films with preferred c-axis orientation along [002] direction. The polycrystallinity increased due to use of aqua-alcoholic precursor solvent. The crystallite size was found to vary from 41.7 nm to 59.4 nm and blue shift in band-gap energy (3.225 eV to 3.255 eV) was observed due to aqua-alcoholic to alcoholic precursor solvent transition. The films deposited using alcoholic precursor solvent exhibited high transmittance (> 92 %) with low dark resistivity (10^{-3} Ω·cm) as compared to aqua-alcoholic precursor solvent. The effect of precursor solvent on resistivity, carrier concentration (η – /cm^3), carrier mobility (μ – cm^{2}V^{-1}s^{-1}), sheet resistance (Ω/□) and figure of merit (Φ_{TC}) is also reported. We recommend ethanol or methanol as a superior precursor solvent over aqua-alcoholic precursor solvent for deposition of device quality ZnO thin films.

Keywords: ZnO thin films, Intermittent spray pyrolysis, XRD, Electrical properties, Optical properties.

DOI: 10.21272/jnep.8(2).02026 PACS numbers: 73.61.Ga, 81.15.Rs, 61.05.C, 73.61.r, 78.66.w

1. INTRODUCTION

Zinc Oxide (ZnO) is one of the most promising II-VI semiconducting materials for optoelectronic applications. It is *n* type, non toxic direct wide band gap material (E_g = 3.3 eV at 300 K) with good electrical conductivity, high excitonic binding energy (60 meV) and high optical transmittance (> 90 %) in the visible range of electromagnetic spectrum. Moreover, it is favourable material for space applications because of its high stability when exposed to hydrogen plasma, high energy radiation and chemical etching [1-4]. ZnO is abundant and has simple crystal growth technology which makes it favoured candidate for low cost applications such as transparent conducting oxide (TCO), solar cells, energy harvesters, antireflection coatings, liquid crystal displays [1-9]. Furthermore, ZnO thin films also find use in gas sensors, ultraviolet sensors and optoelectronics such as: blue/UV light emitting devices, laser, photodetectors, transparent thin-film transistors, field emitters, field effect transistors [10-20].

Extensive research and development efforts on ZnO thin film growth have been underway and device quality films have been deposited successfully by a variety of deposition techniques. These include Chemical Spray Pyrolysis (CSP) [3-8], Metal Organic Chemical Vapor Deposition (MOCVD) [21], Sol-Gel [22], Sputtering [23], Pulsed Laser Deposition (PLD) [24], and Molecular Beam Epitaxy (MBE) [25]. Amongst all these techniques Sputtering, MOCVD, MBE, and PLD are the foremost that have been able to produce device quality films; however, they are expensive, complicated and very hard to be commercialized. On the contrary; the chemical spray pyrolysis (CSP) technique has acquired a considerable attention because it is simple, inexpensive, easy to commercialize and further capable of having large area depositions [3-8]. One of the important and crucial CSP process parameter is precursor solvent which decides the structural, optical and electrical properties of the deposited films. The present work reports the role of precursor solvent on structural and optoelectronic properties of ZnO thin films.

2. EXPERIMENTAL

2.1 ZnO Film Synthesis

ZnO films were synthesized by spray pyrolysis of 0.3 M, 50 ml solution of zinc acetate dihydrate [($Zn(CH_3COO)_2.2H_2O$), Merck, 99.99 % pure] on soda lime glass substrates at deposition temperature of 450 °C. In CSP technique, during film deposition, the precursor solvent should facilitate quick transformation of precursor mist into vapor; hence due to their high volatility ethanol / methanol are favored precursor solvents. In order to investigate the proper solvent for zinc acetate precursor to deposit ZnO thin films with good structural and optoelectronic properties alcoholic and aqua-alcoholic solvents such as (a) ethanol, (b) methanol, (c) ethanol + water (4 : 1) and (d) methanol + water (4 : 1) were used to deposit thin films of ZnO. Double distilled water was used for aqua alcoholic solvents. The water is the best oxidizing agent, however, it was not used as a solvent because under isothermal conditions (> 130 °C) water of crystallization from zinc acetate dihydrate is evaporated (H_2O vapors) into atmosphere causing complete oxidation and results in clean 'c' axis oriented thin films of ZnO below 500 °C [26]. The aerosol droplets reaching the substrate surface undergo an endothermic reaction of zinc acetate with water vapors to form highly adherent and uniform ZnO films. The steps involved in reaction

* c_mahajan9@yahoo.com

 © 2016 Sumy State University

are shown below [3, 7]:

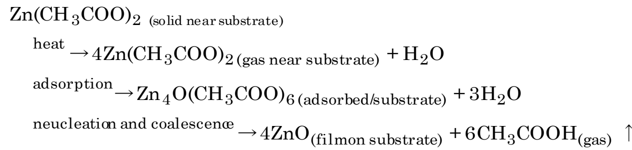

Soda lime glass substrates were chemically and ultrasonically cleaned before deposition and then rinsed in de-ionized water. The precursor solution was intermittently sprayed at 2.5 ml/min flow rate (in spraying cycles of 30 s followed by a break of 30 s to keep steady substrate temperature) onto the hot substrate held at a distance of 30 cm from the spray nozzle. Ultra filtered compressed air (air flow rate – 15 l min^{-1}, air pressure at nozzle – 8 kg/cm^2) was used as a carrier gas. The temperature of substrate heater (3 kW; Make: Baker UK) was maintained constant using an electronic temperature controller unit. Properly insulated housing was used around the substrate to ensure that the deposition temperature remained constant during film synthesis. After deposition the films were annealed at deposition temperature for 10 min for re-crystallization effects to take place.

2.2 Characterization

The X-ray diffraction (XRD) analysis was done for ZnO thin films by using CuK$_\alpha$ radiation ($\lambda = 1.5405$ Å) to investigate the crystal structure and film orientation. The spectral transmittance and absorbance was obtained using UV-VIS-NIR spectrometer (model UV-1650 - PC) in the wavelength of 350 nm to 1100 nm. Hall measurements were performed at room temperature and atmospheric pressure to measure electrical properties of the film with an assumption that the electrical conduction throughout the depth of the film is homogenous. The sheet resistance was measured from the knowledge of resistivity and thickness. The optical transmittance and conductivity of the ZnO thin films are the characteristics to be optimized for its use as a transparent electrode. The dependence of carrier concentration (η – /cm^3) and mobility (μ – cm^{-2}V^{-1}s^{-1}) on precursor solvent is discussed along with variation in sheet resistance (R_s – Ω/□) and figure of merit (Φ_{TC} – Ω^{-1}) for ZnO films in view of their possible applications as transparent conducting coatings and window layers in photovoltaic and optoelectronic devices.

3. RESULTS AND DISCUSSIONS

3.1 Structural Properties

Fig. 1 shows a low angle XRD of CSP deposited ZnO films with precursor dissolved in different solvents in the range of 20°-80° with slow scanning speed (2°/min) and step width of 0.02°). As seen from the XRD, all films are polycrystalline in nature having hexagonal wurtzite structure with most preferred orientation along c- axis [002] direction according to ASTM standards [27]. Other orientations along (100), (101), (102) and (103) crystal planes were also observed; however, their intensities were very weak as compared to the [002] peak. The films deposited from ethanol and subsequently methanol based precursor were most preferably oriented along [002] direction exhibiting higher crystallinity when compared with those deposited using aqua alcoholic solvent for precursor. This may be due to the nucleation process during film formation, if the nucleation is preferred in the initial stage of deposition, a strict improvement in preferred growth is observed [28-30]. Also, the intensity for other orientations was found to be increased when alcoholic solvent was substituted by aqua alcoholic solvent. The high vapor pressure and low surface tension of alcoholic solvent like ethanol or methanol enables the formation of fine droplets during the deposition which favors the crystalline growth of ZnO towards [002] direction. The oxygen necessary for ZnO formation is utilized from the evaporated water vapors from zinc acetate dihydrate or from the surrounding air. Alcohol also acts as a reducing agent, which in turn controls the oxygen deficiency, attributing to the improvement in crystallinity thereby lowering the crystal defect density. The intensity values of XRD peaks for different (h, k, l) planes and measured grain size $d_{[002]}$ of ZnO films deposited using different precursor solvents are listed in Table 1. The classical Scherrer formula [31] as shown in equation (1) was used to estimate the average crystallite size (D) of crystallites / grains for the ZnO films;

$$D = \frac{k\lambda}{\beta \cos\theta} \quad (1)$$

where the constant k is the shape factor usually equal to 1, λ is the wavelength of X-ray, θ is the Bragg's angle and β is the full width of the half maxima (FWHM). Usually the widening of XRD peak is caused by internal stress and defects, so the mean grain size estimated by this method is normally smaller than the actual value.

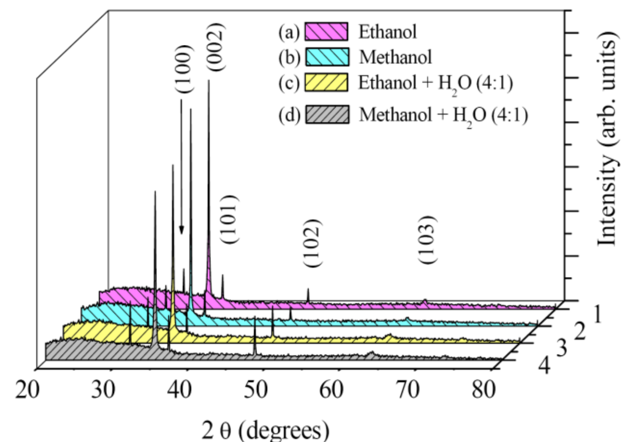

Fig. 1 – XRD patterns of ZnO films deposited by CSP technique using different precursor solvents

3.2 Optical Transmission and Absorption

Fig. 2 shows the measured transmission curves (% T versus λ) for ZnO films deposited using zinc acetate precursor dissolved in different solvents. The inset table in Fig. 2 shows the variation of film thickness and transmittance with variation in precursor solvent. It is observed from Fig. 2 that ZnO films have average

transmittance (73 to 94 %) in the spectral range of 400 nm to 1100 nm. It can also be observed that the optical transmittance for ZnO films obtained using zinc acetate precursor dissolved in alcoholic solvent is maximum. The substantial decrease in transmittance for ZnO films deposited using precursor dissolved in aqua alcoholic solvent is due to poor crystallinity of these films. The superior crystalline structure of ZnO film due to alcoholic solvent is also established through XRD analysis. The films thickness increases due to the use of aqua alcoholic solvent for precursor.

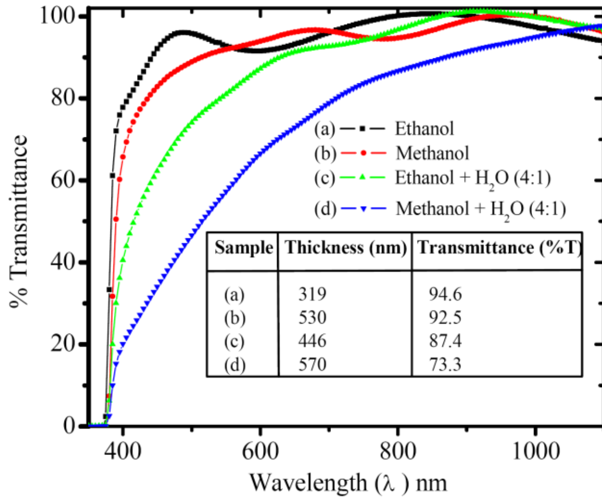

Fig. 2 – Spectral dependence of transmittance for ZnO films synthesized using different precursor solvents. The inset table shows variation of film thickness and transmittance (400 nm-1100 nm)

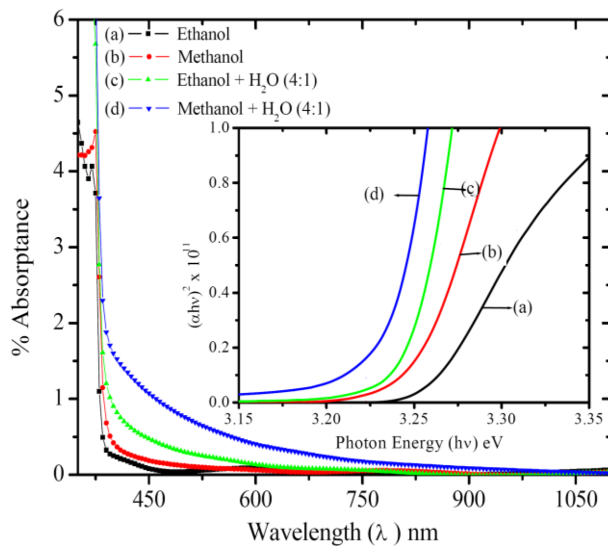

Fig. 3 – Spectral dependence of absorptance for ZnO films synthesized using different precursor solvents. The inset is plot of $(\alpha h\nu)^2$ vs. $h\nu$ of ZnO films

Fig. 3 illustrates the variance of absorption in the range of 350 nm to 1100 nm. It is evident that the absorption coefficient decreases with an increase in wavelength, and a sharp decrease in absorption coefficient, near the band edge for films deposited using precursor dissolved in alcoholic solvent, indicates better crystallinity of the films and lower defect density. The analysis of the transmittance and absorption spectra in the vicinity of the fundamental absorption edge shows that the variation of the absorption coefficient is in accordance with the following relation which implies the direct transitions [5].

$$(\alpha h\nu)^2 = A(h\nu - E_g) \qquad (2)$$

The inset graph in Fig. 3 shows the variation of $(\alpha h\nu^2)$ vs. $h\nu$. The bandgap of the material from graph is x-axis intercept obtained by extrapolating the linear portion of the exponential curve. The energy gap for all the films was found in between 3.225 to 3.255 eV.Table 1 shows the values of crystallite size ($d_{[002]}$) and the band gap energy for ZnO thin films deposited using precursor dissolved in different solvents. The grain size $d_{[002]}$ was observed to be increased when alcoholic solvent was replaced by aqua alcoholic solvent. The variation in energy band gap with crystallite size as seen from Table 1, clearly shows the quantum size effect of decrease in band gap energy due to increase in crystallite size.

Table 1 – Intensity data for different (h, k, l) planes, grain size ($d_{[002]}$) and energy band gap (E_g) of ZnO film deposited using different precursor solvents

Precursor Solvent	$I_{[002]}$	$I_{(100)}$	$I_{(101)}$	$I_{(102)}$	Grain Size $d_{[002]}$ – nm	E_g – eV
Ethanol (Eth.)	5128	905	765	460	41.7	3.255
Methanol (Mth.)	4870	961	797	421	54.8	3.245
Eth.+H_2O (4 : 1)	3994	1033	881	828	49.3	3.240
Mth.+H_2O (4 : 1)	3786	1323	999	987	59.4	3.225

The film thickness was determined via the method developed by Manifacier using the following relation [32].

$$t = \frac{\lambda_1 \lambda_2}{2\left[n_{f\lambda 1}\lambda_2 - n_{f\lambda 2}\lambda_1\right]} \qquad (3)$$

where $n_{f\lambda 1}$ and $n_{f\lambda 2}$ are the refractive indices of the film at two adjacent interference maxima or (minima) at wavelengths $\lambda_1$and λ_2 respectively (usually in this region, n_f is nearly constant: $n_f \sim n_{f\lambda 1} \sim n_{f\lambda 2}$).

3.3 Optoelectronic Properties

3.3a Electrical properties

The Hall Effect (Van der Pauw geometry) electrical measurement technique was used to detect the charge carrier type, carrier concentration, carrier mobility and dark resistivity of the ZnO films. The measurements revealed that all ZnO films were n-type. The variation in film thickness and resistivity of ZnO films deposited using different precursor solvents is shown in Fig. 4. The lowest resistivity (3.74×10^{-3} Ω·cm) was measured for the ZnO film deposited using precursor dissolved in ethanol. This lowest resistivity attributes to good crystallinity and modification of properties of the grain boundaries which results in lower defect density. It can be observed that the resistivity increases when alcoholic solvent is replaced by aqua alcoholic solvent.

The grain boundary effects such as chemisorption of oxygen (O_2^-) molecular ions, poor crystallinity and incorporation of residual nonvolatile organic compounds caused by incomplete decomposition of the metal organic source (zinc acetate) leads to development of potential barriers at grain boundaries and on surface which hamper the electrical transport. However, desorption of chemisorbed oxygen at deposition $T_s > 400$ °C contributes to an excess electron in the ZnO lattice ($O_2^- \to O_2 + e^-$); hence electrical conductivity increases [33, 34]. Moreover, the closed outer 2p shells of O^{2-} ions and empty 4s levels of Zn^{2+} ions in the crystal lattice instigate the neutralization of Zn; which at higher T_s can easily ionize one electron in conduction band increasing the conductivity [35]. The measured resistivity value of 3.74×10^{-3} Ω·cm is in good agreement with those reported in the literature for ZnO thin films [3-7].

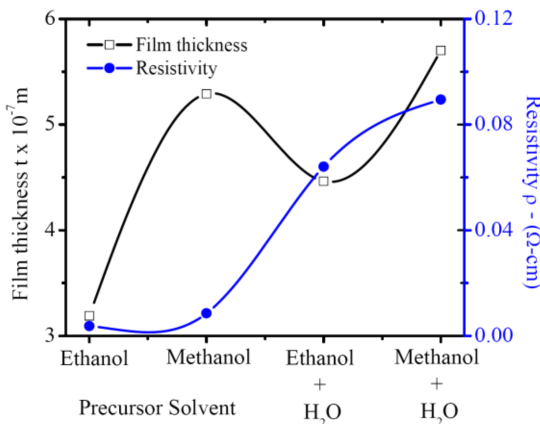

Fig. 4 – Plot shows variation of film thickness (t), resistivity (ρ) of ZnO films synthesized using different precursor solvents

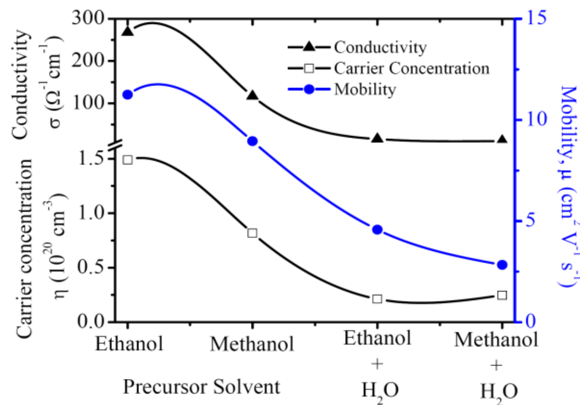

Fig. 5 – Plot shows variation of mobility (μ), conductivity (σ) and carrier concentration (η) in ZnO films synthesized using different precursor solvents

The variation observed in electrical resistivity (σ – $\Omega^{-1}cm^{-1}$), mobility of charge carriers (μ – $cm^{-2}V^{-1}s^{-1}$) and carrier concentration (η – /cm^3) for ZnO films deposited using precursor dissolved in different solvents is shown in Fig. 5. Both carrier concentration and mobility have higher values for alcoholic solvent based ZnO films, whereas, the carrier concentration and mobility decrease substantially when alcoholic solvent is replaced by aqua alcoholic solvent. The highest values of conductivity (268 $\Omega^{-1}cm^{-1}$), carrier concentration (1.49×10^{20}/cm^3) and carrier mobility (11.3 $cm^2V^{-1}s^{-1}$) were measured for ZnO film deposited using ethanol as a precursor solvent. Thus, disorder generated in the lattice seem to be the main cause for the decrease in carrier concentration.

3.3b Figure of Merit

This investigation shows that visible transmittance and electrical resistivity depend significantly on precursor solvent. As already mentioned the purpose is to use ZnO layer as transparent electrode with highest transparency and lowest resistivity. Evaluation of the deposited thin film, as TCO is necessary because under optimum deposition conditions visible transmittance and electrical resistivity depend significantly on film thickness. The electrical resistivity decreases with increasing film thickness however adversely affects its transparency. The figure of merit predicts TCO properties by minimizing the trade-off between electrical resistivity and transparency. Excellent quality TCO film is associated with maximum value of figure of merit. The figure of merit of the films was calculated using the relation proposed by Haacke [36],

$$\Phi_{TC} = \frac{T^{10}}{R_S} \quad (6),$$

where T is the transmittance, R_s the sheet resistance.

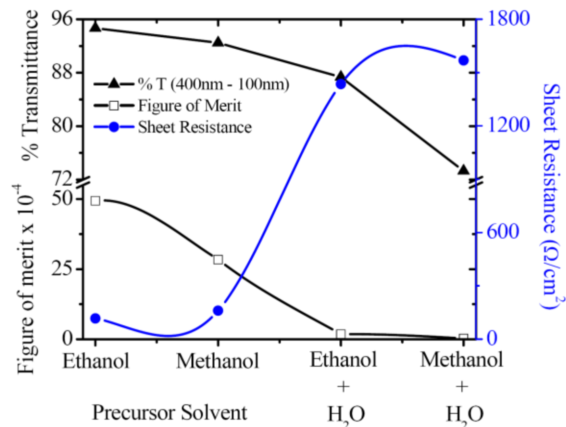

Fig. 6 – Plot shows variation of transmittance (% T), sheet resistance (R_s) and figure of merit (Φ_{TC}) of ZnO films synthesized using different precursor solvents

The variation of sheet resistance (R_s – Ohms/Sq.) and figure of merit (Φ_{TC}) with variation in precursor solvent is shown in Fig. 6. It can be seen that the figure of merit is more for ZnO films obtained by spray pyrolysis of precursor dissolved in alcoholic solvent than that of aqua alcoholic solvent. The highest figure of merit, 4.9×10^{-3} Ω^{-1}, was obtained for a ZnO film deposited using precursor dissolved in ethanol. The corresponding value of sheet resistance is minimum 117 Ω /□ along with maximum transmittance of 94.6 %.

4. CONCLUSIONS

ZnO thin films were deposited by spray pyrolysis

technique using alcoholic and aqua alcoholic solutions of zinc acetate on soda lime glass substrate. The XRD analysis confirmed the polycrystalline nature of films with preferred orientation along [002] plane. The alcoholic precursors lead to synthesis of highly transparent (> 92 %) films with low resistivity (10^{-3} Ω·cm). The aqua-alcoholic to alcoholic precursor solvent transition decreases the crystallite size from 59.4 nm to 41.7 nm and results in blue shift in band-gap energy (3.225 eV to 3.255 eV). We recommend ethanol or methanol as a precursor solvent over aqua-alcoholic precursor solvents for deposition of device quality transparent conducting thin films of ZnO.

ACKNOWLEDGEMENTS

This work was financially supported by Board for College and University Development (BCUD), Savitribai Phule University of Pune, Pune, Maharashtra.

REFERENCES

1. D.C. Look, *Mater. Sci. Eng. B: Solid-State Mater. Adv. Technol.* **80**, 383 (2001).
2. S.O. Kucheyev, J.S. Williams, C. Jagadish, J. Zou, C. Evans, A.J. Nelson, A.V. Hamza, *Phys. Rev. B* **67**, 094115 (2003).
3. F. Paraguay D., W. Estrada L., D.R. Acosta N., E. Andrade, M. Miki-Yoshida, *Thin Solid Films* **350**, 192 (1999).
4. D.J. Goyal, C. Agashe, M.G. Takwale, B.R. Marathe, V.G. Bhide, *J. Mater. Sci.* **27**, 4705 (1992).
5. A. Ashour, M.A. Kaid, N.Z. El-Sayed, A.A. Ibrahim, *Appl. Surf. Sci.* **252**, 7844 (2006).
6. C.M. Mahajan, M.G. Takwale, *Curr. Appl. Phys.* **13**, 2109 (2013).
7. C.M. Mahajan, M.G. Takwale, *J. Alloy. Compd.* **584**, 128 (2014).
8. M.T. Mohammad, A.A. Hashim, M.H. Al-Maamory, *Mater. Chem. Phys.* **99**, 382 (2006).
9. G.A. Zhu, R.S. Yang, S.H. Wang, Z.L. Wang, *Nano Lett.* **10**, 3151 (2010).
10. M. Law, L.E. Greene, J.C. Johnson, R. Saykally, P. Yang, *Nat. Mater.* **4**, 455 (2005).
11. V.R. Shinde, T.P. Gujar, C.D. Lokhande, *Sensor. Actuat. B* **120**, 551 (2007).
12. G. Hua, Y. Zhang, J. Zhang, X. Cao, W. Xu, L. Zhang, *Mater. Lett.* **62**, 4109 (2008).
13. Z.W. Pan, Z.R. Dai, Z.L. Wang, *Science* **291**, 1947 (2001).
14. B.Y. Oh, M.C. Jeong, T.H. Moon, W. Lee, J.M. Myoung, J.Y. Hwang, D.S. Seo, *J. Appl. Phys.* **99**, 124505 (2006).
15. L. Luo, Y.F. Zhang, S.S. Mao, L.W. Lin, *Sensor. Actuat. A-Phys.* **127**, 201 (2006).
16. R.S. Aga, D. Jowhar, A. Ueda, Z. Pan, W. E. Collins, R. Mu, K.D. Singer, J. Shen, *Appl. Phys. Lett.* **91**, 232108 (2007).
17. Y.B. Li, F. Della Valle, M. Simonnet, I. Yamada, J.J. Delaunay, *Nanotechnology* **20**, 045501 (2009).
18. W. Wu, S. Bai, N. Cui, F. Ma, Z. Wei, Y. Qin, E. Xie, *Sci. Adv. Mater.* **2**, 402 (2010).
19. J.H. Ahn, H.S. Kim, K.J. Lee, S. Jeon, S.J. Kang, Y.G. Sun, R.G. Nuzzo, J.A. Rogers, *Science* **314**, 1754 (2006).
20. A. Javey, S. Nam, R.S. Friedman, H. Yan, C.M. Lieber, *Nano Lett.* **7**, 773 (2007).
21. W. Lee, M.C. Jeong, J.M. Myoung, *Acta Mater.* **52**, 3949 (2004).
22. J.H. Lee, K.H. Ko, B.O. Park, *J. Crystal Growth* **247**, 119 (2003).
23. E. Fortunato, V. Assunção, A. Gonçalves, A. Marques, H. Águas, L. Pereira, I. Ferreira, R. Martins, *Thin Solid Films* **451-452**, 443 (2004).
24. D. Valerini, A.P. Caricato, M. Lomascolo, F. Romano, A. Taurino, T. Tunno, M. Martino, *Appl. Phys. A* **93**, 729 (2008).
25. K. Ogata,T. Komuro, K. Hama, K. Koike, S. Sasa, M. Inoue, M. Yano, *Phys. Status Solidi B* **241**, 616 (2004).
26. A. Djelloul, K. Bouzid, F. Guerrab, *Turk. Jour. Phys.* **32**, 49 (2008).
27. Powder Diffraction File, Data Card 5-644, 3c PDS International Centre for Diffraction Data, Swarthmore, PA.
28. C.M. Mahajan, A.G. Godbole, S.P. Gumfekar, S.H. Sonawane, M.G. Takwale, *Adv. Mater. Res.* **67**, 103 (2009).
29. C.M. Mahajan, M.G. Takwale, *International Workshop on Physics of Semiconductor Devices*, 911 (2007).
30. B. Elidrissi, M. Addou, M. Regragui, C. Monty, A. Bougrine, A. Kachouane, *Thin Solid Films* **379**, 23 (2000).
31. H.P. Klung, L.E. Alexander, *X-ray Diffraction Procedures For Polycrystalline and Amorphous Materials, 2nd Edition* (Wiley: New York: 1974).
32. J.C. Manifacier, *Thin Solid Films* **90**, 297 (1982).
33. Shih-Chia Chang, *J. Vac. Sci. Technol.* **17** No 1, 366 (1980).
34. Y. Fujita, T. Kwan, *J. Res. Inst. Catal.* **7**, 24 (1959).
35. L.V. Azaroff, J.J. Brophy, *Electronic process in materials* (McGraw-Hill: New York: 1963).
36. G. Haacke, *J. Appl. Phys.* **47**, 4086 (1976).